Quantitative analysis of FMS images to determine pore space characteristics in a subaerial basaltic lava flow

M. Linek, A. Bartetzko, R. Pechnig: Applied Geophysics, RWTH Aachen;
C. Breitkreuz: Geology Department, TU Bergakademie Freiberg
H. Lindner: Geophysics Department, TU Bergakademie Freiberg

Introduction

High resolution electrical images of borehole walls have been developed for qualitative recognition and quantitative extraction of structural (strike and dip) and depositional (vugs and bedding) features (Prensky, 1999). This study is focused on Formation MicroScanner (FMS) images of Ocean Drilling Program Hole 917A to quantify the internal morphological characteristics of a basaltic lava flow. Digital image analysis software converts qualitative information of dynamically processed images into quantitative parameter. Geometric features of vesicles and fractures such as size, shape and distribution will be studied and integrated with logging data. A first attempt was accomplished to derive elastic properties of this basaltic lava flow from FMS images by calculating seismic velocities. Here, an object oriented finite element method software is used to calculate the compressional wave velocity of the basalt depending on different filling characteristics.

Methods

Subaerial lava flows show internal flow zonation by characteristic log responses. Small scale variations of physical properties are mainly controlled by vesicularity. In general, four units can be distinguished using log responses within one single flow. Zonation is indicated by stepped trends and alternating gradients in the most significant logs such as bulk density, compressional wave velocity, deep induction, spherically focused resisitivity and neutron porosity (Bücker et al., 1998; Delius et al., 2003, 1995; Planke, 1994). These characteristic log responses were used to select a single lava flow ranging from 432.5 mbsf (metres below sea floor) up to 449.5 mbsf. The corresponding dynamically processed FMS images were cut in 20 cm depth intervals for digital image analysis. This depth interval was chosen due to similar tools' sampling rate.

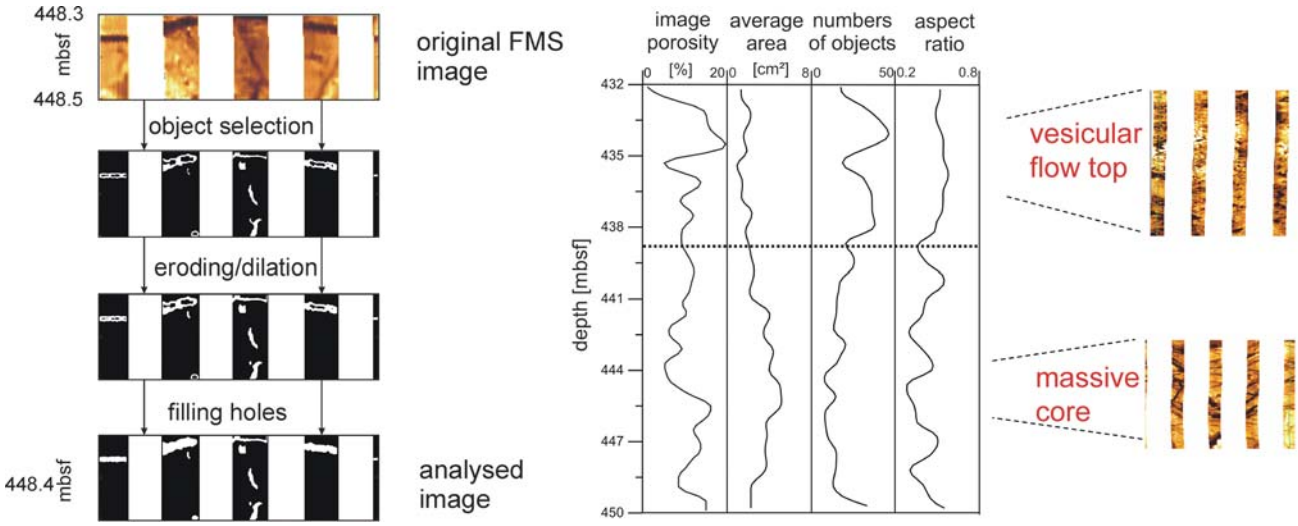

Figure 1: Stages involved in digital image analysis: original FMS image is split into 20 cm depth interval, translated into binary images through colour selection, edited and finally filled. The plot of the righthand side represents the results of digital image analysis.

The process of image analysis involved three stages to provide appropriate binary images for automatical analysis with digital image analysis software KS400 (Kontron Elektronik, 1995) as shown in Figure 1. At first, objects of interest have been selected by a defined colour threshold range to convert colour images into binary ones. The desired conductive objects such as vesicles and fractures appear as dark brown spots in contrast to their light and yellowish resistive surrounding. Once the colour threshold was manually adapted and refined to each image, all objects within this limit were selected. In the next stage, the selected objects were edited by eroding or dilation: large objects were reduced by deleting marginal pixel. Consequently, adjacent objects were separated. This step also included rounding of angular objects. As shown in Figure 1, objects had to be filled in the third stage. Both editing stages were done to adapt the third binary image to the original FMS image as good as possible. Finally, the following geometric parameters have been specified and automatically measured from the third binary image: object's area, minor and major ellipse axis. Calculated data from every image interval was averaged and tabulated to obtain only one value for all parameters measured. The average values have been depth related to the middle of each image. An objects aspect ratio was calculated by the ratio between minor and major ellipse axis. It was weighted according to the object area proportionally to the total area. The percentage of the total object area to the entire pad area was determined as image porosity. Elastic properties were studied based

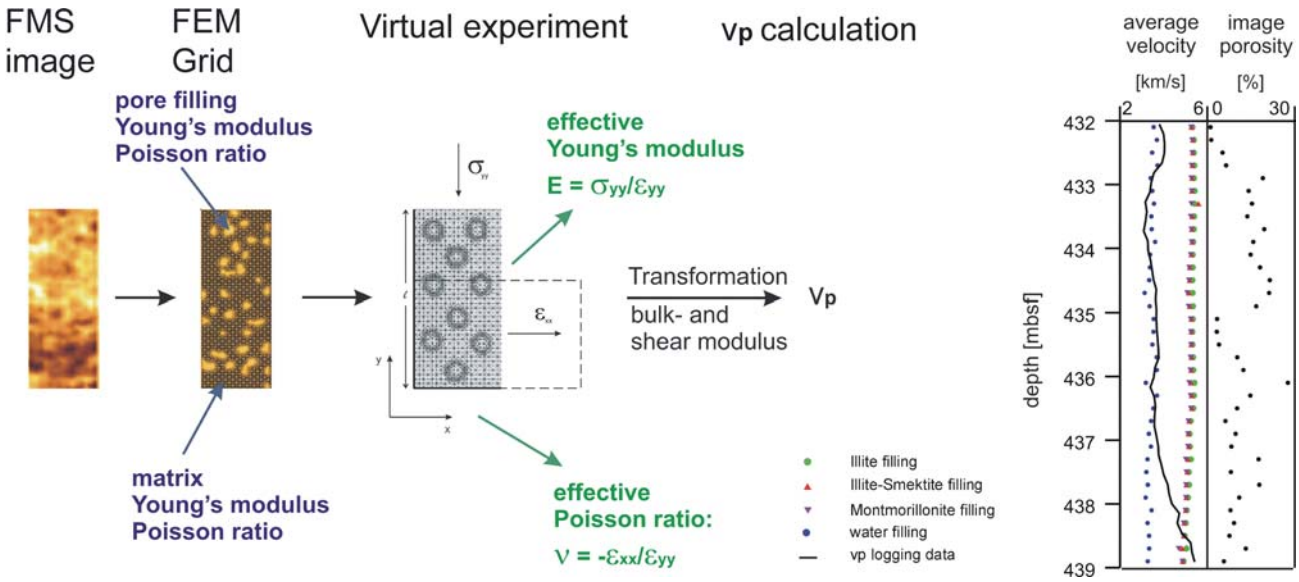

Figure 2: Modelling the elastic behaviour to derive compressional wave velocity from FMS images in dependence of different pore fillings. The plot of the righthand side reveals the mean of compressional wave velocity calculation.

on vesicular FMS images and were used to derive the compressional wave velocity in reliance on different pore fillings. FMS image microstructure was converted into a finite element grid (see Figure 2). The Poisson ratio and the Young's modulus were assigned to pore filling and basaltic matrix. Object oriented finite element software OOF can be used to perform virtual mechanical experiments (Carter et al., 2000). Uniaxial compression was tested to determine the elastic constants for stress σ and strain ε which were observed and output as tensors. Tensors are used to determine effective Young's modulus and Poisson ratio which in turn were transformed to bulk K and shear modulus μ.

Results

Results of digital image analysis are displayed in Figure 1. In contrast to logging data, where four flow units could be recognised, only two distinctive flow units *vesicular flow top* and *massive core* were obtained. Image unit *vesicular flow top* is characterised by an almost constant aspect ratio > 0.5 and a high number of objects on average $\pm$ 40, except between 434.5 mbsf and 434.5 mbsf. Image analysis also revealed a more or less constant average object area of about 2 cm^2. Image porosity reaches values up to 20 %. Image unit *massive core* is characterised by a downward decreasing weighted aspect ratio, which sometimes reaches values lower than 0.2 and a decrease in the numbers of objects curve. There is also a strong downward increase in average area. Vesicular images were used to derive compressional wave velocity in dependence

on different pore fillings. As displayed in Figure 2, the mean value obtained for different clay ($\approx$ 5.8 km/s) and water fillings ($\approx$ 3.8 km/s) was integrated with in-situ compressional wave velocity. Comparison of calculated and in-situ velocity showed a good agreement for the assumed water filling, so that the vesicular part of this lava flow may be interpreted as water filled.

Conclusion

FMS images of a subaerial basaltic lava flow were investigated by digital image analysis. Image results allow a distinction between vesicular and massive flow part. Differences between those flow units are mainly based on decrease in number of objects, object's aspect ratio and average area throughout the flow. A first attempt was accomplished to derive compression wave velocity from vesicular image data. Different pore fillings were used to determine elastic properties. A good agreement between assumed water filling and compressional wave velocity logging data indicated mainly water filled vesicles.

References

Bücker, C., Delius, H., Wohlenberg, J., and LEG 163 Shipboard Scientific Party (1998). Physical signature of basaltic volcanics drilled on the northeast Atlantic volcanic rifted margin. In Harvey, P. and Lovell, M., editors, *Core-Log Integration*, volume 136 of *Special Publications*, pages 363–374. The Geological Society, London.

Carter, C., Langer, S., and Fuller, E. (2000). *The OOF Manual: Version 1.0.8.6.* National Institute of Standards and Technology.

Delius, H., Brewer, T., and Harvey (2003). Evidence for textural and alteration changes in basaltic lava flows using variations in rock magnetic properties (ODP Leg 183). *Tectonophysics*, 371:111–140.

Delius, H., Bücker, C., and Wohlenberg, J. (1995). Significant log responses of basaltic lava flows and volcaniclastic sediments in ODP Hole 642E. *Scientific Drilling*, 5:217–226.

Kontron Elektronik (1995). *Kontron Elektronik Imaging System KS400 - Manual.* Carl Zeiss Jena.

Planke, S. (1994). Geophysical responses of flood basalts from analysis of wire line logs: Ocean Drilling Program Site 642, Vøring volcanic margin. *Journal of Geophysical Research*, 99:9279–9296.

Prensky, S. (1999). Advances in borhole imaging technology and applications,. In Lovell, M. A., Williamson, G., and Harvey, P., editors, *Borehole Imaging: applications and case histories*, volume 159 of *Special Publications*, pages 1–43. The Geological Society, London.